

## Nonheme Fe<sup>IV</sup>O Complexes That Can Oxidize the C–H Bonds of Cyclohexane at Room Temperature

József Kaizer,<sup>†</sup> Eric J. Klinker,<sup>†</sup> Na Young Oh,<sup>‡</sup> Jan-Uwe Rohde,<sup>†</sup> Woon Ju Song,<sup>‡</sup> Audria Stubna,<sup>§</sup> Jinheung Kim,<sup>||</sup> Eckard Münck,<sup>\*,§</sup> Wonwoo Nam,<sup>\*,‡</sup> and Lawrence Que, Jr.<sup>\*,†</sup>

Department of Chemistry and Center for Metals in Biocatalysis, University of Minnesota, Minneapolis, Minnesota 55455, Department of Chemistry and Division of Nano Sciences, Ewha Womans University, Seoul 120-750, Korea, Department of Chemistry, Carnegie Mellon University, Pittsburgh, Pennsylvania 15213, and Department of Chemical Technology, Changwon National University, Changwon 641-773, Korea

Received July 15, 2003; E-mail: que@chem.umn.edu

Postulated mechanisms for the functionalization of aliphatic C–H bonds by mononuclear nonheme iron(II) enzymes often invoke C–H bond cleavage by an Fe<sup>IV</sup>=O intermediate that is generated by dioxygen activation.<sup>1,2</sup> Such transformations include the hydroxylation of prolyl or asparagine residues by enzymes that are involved in sensing hypoxia in mammalian cells,<sup>3</sup> ring-forming reactions in the biosynthesis of  $\beta$ -lactam antibiotics such as penicillin, cephalosporin, and clavulanic acid,<sup>4</sup> and the first step in the biodegradation of the herbicide 2,4-D.<sup>5</sup> The general features of these transformations parallel the mechanism widely accepted for heme enzymes such as cytochrome P450, except that the nonheme enzymes employ an Fe<sup>II</sup>/Fe<sup>IV</sup>=O redox couple in place of the formally Fe<sup>III</sup>/Fe<sup>V</sup>=O couple associated with heme enzymes. In support, direct spectroscopic evidence for an iron(IV) intermediate in this class of enzymes has just been reported for the 2-oxoglutarate-dependent enzyme TauD.<sup>6</sup> While it is well established that the high-valent heme intermediate, best described as [Fe<sup>IV</sup>(O)-(porphyrin  $\pi$ -cation radical)]<sup>+</sup>, can hydroxylate the C–H bonds of cyclohexane ( $D_{C-H} \approx 99.3$  kcal/mol),<sup>7</sup> the proposed mechanisms for nonheme enzymes raise the interesting question as to whether the corresponding one-electron reduced Fe<sup>IV</sup>=O unit in a nonheme ligand environment has sufficient oxidizing power to cleave aliphatic C–H bonds as strong as those found on the C-3 and C-4 positions of proline. We recently reported the high-yield generation of synthetic oxoiron(IV) complexes using tetradentate N4 ligands such as the macrocyclic TMC and the tripodal TPA ligands<sup>8,9</sup> and obtained a high-resolution X-ray structure of the former.<sup>9a</sup> While the TMC complex can effect oxygen-atom transfer only to PPh<sub>3</sub> at –40 °C, the TPA complex is able to epoxidize cyclooctene at this temperature. We now report the synthesis and characterization of corresponding Fe<sup>IV</sup>=O complexes of the pentadentate N5 ligands N4Py and Bn-tpen.<sup>8</sup> Most striking of their properties are their higher temperature stability and their ability to hydroxylate C–H bonds as strong as those in cyclohexane.

Treatment of [Fe<sup>II</sup>(N4Py)(CH<sub>3</sub>CN)]<sup>2+</sup> 10 with excess solid PhIO in CH<sub>3</sub>CN at 25 °C affords a green species **1** that persists for several days ( $t_{1/2} \approx 60$  h). The green color is associated with a band at 695 nm ( $\epsilon$  400 M<sup>-1</sup> cm<sup>-1</sup>) (Figure 1) with a shoulder near 800 nm. Like treatment of [Fe<sup>II</sup>(Bn-tpen)(O<sub>3</sub>SCF<sub>3</sub>)]<sup>+</sup> 11 also affords a green species **2** with  $\lambda_{max}$  at 739 nm ( $\epsilon$  400 M<sup>-1</sup> cm<sup>-1</sup>) and a shoulder near 900 nm, but this species is less stable ( $t_{1/2} \approx 6$  h). Similar near-IR bands have been reported for [Fe<sup>IV</sup>(O)(TMC)(CH<sub>3</sub>CN)]<sup>2+</sup> (**3**) ( $\lambda_{max}$  820 nm) and [Fe<sup>IV</sup>(O)(TPA)(CH<sub>3</sub>CN)]<sup>2+</sup> (**4**) ( $\lambda_{max}$  720 nm).<sup>9</sup>

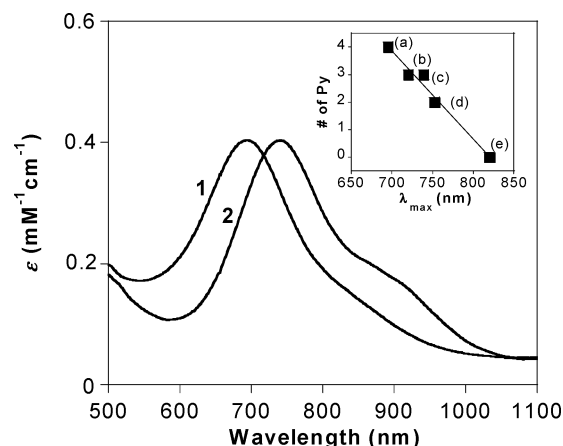


**Figure 1.** Electronic spectra of **1** and **2** in CH<sub>3</sub>CN at 25 °C. Inset: Correlation between the number of pyridine ligands and the absorption maxima of [Fe<sup>IV</sup>(O)(L)] complexes (L = N4Py (a), Bn-tpen (b), TPA (c), BPMCN (d), and TMC (e)).

The nature of these green species can be established by other spectroscopic techniques. Thus, high-resolution electrospray mass spectrometry reveals respective molecular ions at  $m/z$  538.0559 and 644.1227, mass values fully consistent with their formulation as {[Fe<sup>IV</sup>(O)(N4Py)](ClO<sub>4</sub>)<sup>+</sup> (**1**) ( $m/z$  calcd 538.0583) and {[Fe<sup>IV</sup>(O)(Bn-tpen)](O<sub>3</sub>SCF<sub>3</sub>)<sup>+</sup> (**2**) ( $m/z$  calcd 644.1247) ions (Figure S1, Supporting Information). Mössbauer spectra confirm the presence of the iron(IV) state in both complexes, as indicated by  $\Delta E_Q$  and  $\delta$  values of 0.93 mm/s and –0.04 mm/s for **1** and 0.87 and 0.01 mm/s for **2** (Figure S2, Supporting Information). The isomer shifts are similar or identical to the 0.01 mm/s value associated with **4**. Thus, **1** and **2** belong to an emerging class of low-spin Fe<sup>IV</sup>=O complexes with nonheme ligand environments with a near-IR spectral signature. As illustrated in the inset of Figure 1, the  $\lambda_{max}$  values of the five established oxoiron(IV) complexes correlate well with the number of pyridine ligands. The observation that more pyridine ligands give rise to higher energy transitions supports the notion that this near-IR band is ligand field in character, rather than charge transfer in origin,<sup>9</sup> but more detailed investigations (in progress) are needed to establish the spectral assignment.

Although closely related to **4**, **1** and **2** are thermally more stable, presumably due to the pentadentate ligands in the latter two complexes. Despite their higher room-temperature stability, **1** and **2** react with a number of hydrocarbons at room temperature. Figure 2 shows that the addition of 25 equiv of triphenylmethane results in a rapid decay of **1** concomitant with the nearly quantitative appearance of its iron(II) precursor ( $\lambda_{max}$  450 nm) with an isosbestic point at 560 nm. Ph<sub>3</sub>C–OH is obtained in 90% yield, demonstrating

<sup>†</sup> University of Minnesota.

<sup>‡</sup> Ewha Womans University.

<sup>§</sup> Carnegie Mellon University.

<sup>||</sup> Changwon National University.

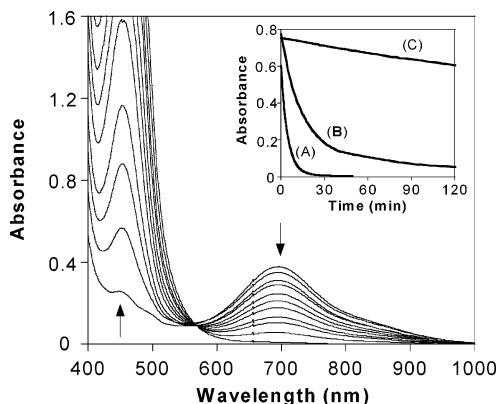


**Figure 2.** Conversion of **1** (1 mM) to its iron(II) precursor in  $\text{CH}_3\text{CN}$  upon addition of  $\text{Ph}_3\text{CH}$  at 25 °C. Inset: time course of the decay of **1** (2 mM) monitored at 695 nm upon addition of 0.1 M  $\text{Ph}_3\text{CH}$  (A), 0.5 M  $\text{PhEt}$  (B), and 0.5 M  $\text{PhEt-d}_{10}$  (C) in  $\text{CH}_3\text{CN}$  at 25 °C.

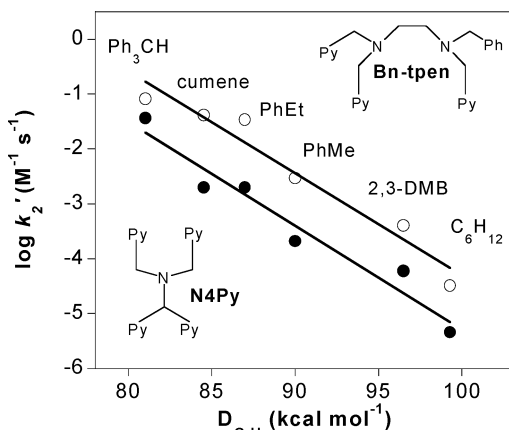


**Figure 3.** Correlation between the C–H bond dissociation energies of various hydrocarbons and  $\log k_2'$  (25 °C) for their reactions with **1** (●) or **2** (○);  $k_2'$  is the second-order rate constant divided by the number of equivalent C–H bonds on the substrate. See Supporting Information for further details.

that **1** is capable of effective oxygen-atom insertion into an activated C–H bond. Complex **1** also reacts with other substrates having stronger C–H bonds at slower rates and with lower yield (Table S1, Supporting Information). As shown in Figure 3, there is a linear correlation between  $\log k_2'$  and C–H bond dissociation energy ( $D_{\text{C-H}}$ ) from  $\text{Ph}_3\text{C-H}$  to cyclohexane. A similar plot is observed for **2**, but with faster rates of reactions, in line with its lower stability. Analogous linear correlations have been obtained for  $[\text{Fe}^{\text{III}}(\text{Py}_5)(\text{OMe})_2]^{2+}$  and  $[\text{Ru}^{\text{IV}}(\text{O})(\text{bpy})_2(\text{py})]^{2+}$ ,<sup>12</sup> but **1** and **2** are clearly capable of oxidizing hydrocarbons with stronger C–H bonds.

The inset in Figure 2 compares the decay rates of **1** in the presence of  $\text{Ph}_3\text{CH}$  and ethylbenzene, showing the slower reaction of the substrate with the stronger C–H bond. More significantly, its  $d_{10}$  isotopomer shows a large kinetic isotope effect of 30. The corresponding experiments for **2** affords a KIE of 50. Such high KIE values are similar to those reported for the reaction of ethylbenzene with  $[\text{Fe}_2\text{O}_2(\text{TPA})_2]^{3+}$  at  $-40$  °C<sup>13</sup> and the hydroxylation of cyclohexane by  $[\text{Fe}(\text{O})(\text{porphyrin})]^+$  at 20 °C,<sup>14</sup> but this is the first instance of a large KIE observed at ambient temperature

for a synthetic nonheme iron complex. Such large isotope effects have been observed for hydrogen atom abstraction reactions by the iron(IV) intermediates of the monoiron TauD<sup>6b</sup> and the diiron enzyme methane monooxygenase,<sup>15</sup> for which hydrogen tunneling mechanisms may be involved. The observation of a large kinetic isotope effect for a synthetic mononuclear  $\text{Fe}^{\text{IV}}(\text{O})$  species provides the opportunity to explore this phenomenon with a simple system.

In summary, we have obtained and characterized nonheme oxoiron(IV) complexes of two pentadentate ligands with properties similar to the closely related tetradentate TPA counterpart reported earlier. However, unlike the TPA complex, the pentadentate complexes have considerably longer lifetimes at room temperature. This greater thermal stability has allowed the hydroxylation of alkanes with C–H bonds as strong as 99.3 kcal/mol to be observed with large deuterium KIEs. These observations lend strong credence to postulated mechanisms of mononuclear nonheme iron enzymes that invoke the intermediacy of oxoiron(IV) species.

**Acknowledgment.** This work was supported by the National Institutes of Health (GM-33162 to L.Q. and GM-22701 to E.M.), the Ministry of Science and Technology of Korea through the Creative Research Initiative Program (W.N.), and an NSF graduate fellowship to A.S.

**Supporting Information Available:** Detailed procedures, figures of electrospray mass spectra and Mössbauer spectra of **1** and **2**, and table listing results of hydrocarbon oxidation experiments associated with Figure 3 (PDF). This material is available free of charge via the Internet at <http://pubs.acs.org>.

## References

- Que, L., Jr.; Ho, R. Y. N. *Chem. Rev.* **1996**, *96*, 2607–2624.
- Solomon, E. I.; Brunold, T. C.; Davis, M. I.; Kemsley, J. N.; Lee, S.-K.; Lehnert, N.; Neese, F.; Skulan, A. J.; Yang, Y.-S.; Zhou, J. *Chem. Rev.* **2000**, *100*, 235–349.
- Bruick, R. K.; McKnight, S. L. *Science* **2001**, *294*, 1337–1340.
- Schofield, C. J.; Zhang, Z. *Curr. Opin. Struct. Biol.* **1999**, *9*, 722–731.
- Liu, A.; Ho, R. Y. N.; Que, L., Jr.; Ryle, M. J.; Phinney, B. S.; Hausinger, R. P. *J. Am. Chem. Soc.* **2001**, *123*, 5126–5127.
- (a) Price, J. C.; Barr, E. W.; Tirupati, B.; Bollinger, J. M., Jr.; Krebs, C. *Biochemistry* **2003**, *42*, 7497–7508. (b) Price, J. C.; Barr, E. W.; Tirupati, B.; Krebs, C.; Bollinger, J. M., Jr. *J. Am. Chem. Soc.* **2003**, *125*, 13008–13009.
- Groves, J. T.; Han, Y.-Z. In *Cytochrome P450: Structure, Mechanism, and Biochemistry*, 2nd ed.; Ortiz de Montellano, P. R., Ed.; Plenum Press: New York, 1995; pp 3–48.
- Ligand abbreviations used: Bn-tpen, *N*-benzyl-*N,N,N'*-tris(2-pyridylmethyl)-1,2-diaminoethane; bpmcn, *N,N'*-dimethyl-*N,N'*-bis(2-pyridylmethyl)-*trans*-1,2-diaminocyclohexane; bpy, 2,2'-bipyridine; N4Py, *N,N*-bis(2-pyridylmethyl)-bis(2-pyridyl)methylamine; py, pyridine; Py5, 2,6-bis(bis(2-pyridyl)methoxymethyl)pyridine; TMC, 1,4,8,11-tetramethylcyclam; TPA, tris(2-pyridylmethyl)amine.
- (a) Rohde, J.-U.; In, J. H.; Lim, M. H.; Brennessel, W. W.; Bukowski, M. R.; Stubna, A.; Münck, E.; Nam, W.; Que, L., Jr. *Science* **2003**, *299*, 1037–1039. (b) Lim, M. H.; Rohde, J.-U.; Stubna, A.; Bukowski, M. R.; Costas, M.; Ho, R. Y. N.; Münck, E.; Nam, W.; Que, L., Jr. *Proc. Natl. Acad. Sci. U.S.A.* **2003**, *100*, 3665–3670.
- Lubben, M.; Meetsma, A.; Wilkinson, E. C.; Feringa, B.; Que, L., Jr. *Angew. Chem., Int. Ed. Engl.* **1995**, *34*, 1512–1514.
- See Supporting Information for details on synthesis and characterization.
- (a) Goldsmith, R. C.; Jonas, R. T.; Stack, D. P. *J. Am. Chem. Soc.* **2002**, *124*, 83–96. (b) Bryant, J. R.; Mayer, J. M. *J. Am. Chem. Soc.* **2003**, *125*, 10351–10361.
- Kim, C.; Dong, Y.; Que, L., Jr. *J. Am. Chem. Soc.* **1997**, *119*, 3635–3636.
- Sorokin, A. B.; Khenkin, A. M. *J. Chem. Soc., Chem. Commun.* **1990**, 45–46.
- Nesheim, J. C.; Lipscomb, J. D. *Biochemistry* **1996**, *35*, 10240–10247.

JA037288N